Available online at www.sciencedirect.com
SCIENCE DIRECT®
Journal of Power Sources 131 (2004) 261–269
JOURNAL OF POWER SOURCES
www.elsevier.com/locate/jpowsour

Prevention of SOFC cathode degradation in contact with Cr-containing alloy

K. Fujita*, K. Ogasawara, Y. Matsuzaki, T. Sakurai

Technical Research Institute, Tokyo Gas Co., Ltd., 16-25 Shibaura, 1-chome, Minato-ku, Tokyo 105-0023, Japan

Received 3 October 2003; accepted 16 December 2003

Abstract

The effects of coating materials on Cr-containing alloy separators were examined for preventing the degradation of solid oxide fuel cell (SOFC) performance. Various oxide materials (YSZ, Y_2O_3, La_2O_3, $LaAlO_3$ and (La,Sr)CoO_3, LSCO) were coated on the alloys, and investigated for the degree of Cr-poisoning using a half-cell measurement method. In these oxides, (La,Sr)CoO_3 coating was found to be effective for preventing the degradation. The LSCO-coated alloy was analyzed by X-ray diffractometry (XRD), scanning electron microscope (SEM) and energy dispersion X-ray (EDX) analysis. The interface between the cathode and the electrolyte was examined by electron probe micro analysis. Consequently, it was proved that a LSCO coating controls the growth of the Cr_2O_3 oxide layer on the Cr-containing alloy surface. And the effects of LSCO coating were further confirmed by a single-cell stack test.

Keywords: Solid oxide fuel cell; Cr-poisoning; Metallic separator; Half-cell

1. Introduction

The development of medium-temperature operable solid oxide fuel cells (SOFCs) is promising to reduce manufacturing costs by using alloy interconnects [1,2]. Considering the electrical resistivity of the oxide layer on the alloy, a Cr-containing alloy is used for the SOFC separators. However, Cr-containing alloys cause degradation of the SOFC performance due to Cr-poisoning during long-term operation [3]. Aiming at the prevention of cathode poisoning from Cr-containing vapor, alloy materials coated by several kinds of oxide materials were examined in half-cell and single-cell stack tests.

2. Experimental

2.1. Preparation method for oxide-coated alloy

As Cr-containing alloys, ZMG232 (Hitachi Metals Co., Ltd., Japan) and SUS430 (Nisshin Steel Co., Ltd., Japan) were used. The chemical compositions of the alloys are listed in Table 1. Various reagents (LSCO: Toshima Manufacturing Co., Ltd., the others: Symetrix Corp.) listed in Table 2 were spin-coated on the surface of ZMG232 plates, and then dried at 373 K for 2 h. After repeating this process three times, the coated ZMG232 plates were annealed at 1173 K. In addition, the LSCO coating on the ZMG232 and SUS430 was prepared also by an electron beam physical vapor deposition (EBPVD, Fig. 1) technique. The substrate temperature, accelerating voltage and evaporation rate of EBPVD were 573 K, 6 kV and 10 Å/s, respectively. The as-deposited samples were annealed at 1073 K for 2 h in air. Both as-deposited and annealed samples were analyzed by X-ray diffractometry (XRD, Bruker Axs Inc. M12X).

2.2. Half-cell tests

The degrees of Cr-poisoning were investigated by using a $La_{0.6}Sr_{0.3}CrO_3$ (LSC) ceramic separator, and the spin-coated and EBPVD alloy separators. The schematic illustration of a half-cell measurement method is shown in Fig. 2. We used cylindrical pellets of electrolyte of 2 cm in diameter and 2 mm in thickness. For the reference electrode, a platinum paste of 0.3 mm in size was printed at the perimeter of the pellet. For the cathode, $La_{0.6}Sr_{0.4}MnO_3$ (LSM), which was reported to easily lose activity by Cr-poisoning [4], was screen-printed on the center of the electrolyte surface, and sintered at 1423 K for 2 h. For the counter electrode, a platinum paste was screen-printed on the other side of cathode, and sintered at 1273 K for 10 h. Pt-mesh was set

* Corresponding author.
E-mail address: f-fujita@tokyo-gas.co.jp (K. Fujita).

0378-7753/$ – see front matter © 2004 Elsevier B.V. All rights reserved.
doi:10.1016/j.jpowsour.2003.12.051

Table 1
Chemical compositions of the Cr-containing alloys used in this study

	Chemical composition (wt.%) of the chromium-containing alloy											
	Cr	Fe	Ni	Mn	Si	C	P	S	Al	La	Zr	Cu
SUS430 Nisshin Steel Co., Ltd.	16.03	82.27	0.29	0.91	0.42	0.06	0.018	0.001	–	–	–	–
ZMG232 Hitachi Metals Co., Ltd.	22.00	76.48	0.26	0.48	0.36	0.02	–	–	0.14	0.04	0.22	–

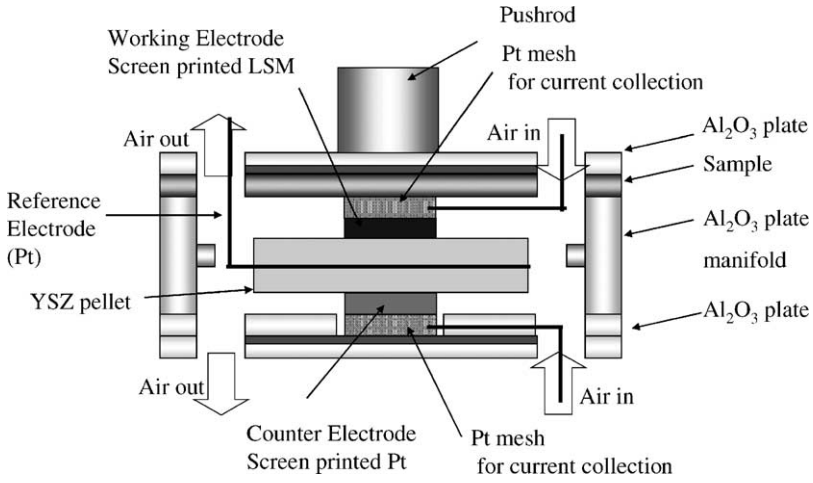

Fig. 1. Schematic representation of an apparatus used for electron beam physical vapor deposition.

between the cathode and the alloy separator. The flow rate of air was set at 2 l/min, in order to supply sufficient dry air into the half-cell. An overvoltage and ohmic resistance were measured under a current density of 0.3 A/cm^2 at 1073 K.

At first, the half-cell test using $La_{0.6}Sr_{0.3}CrO_3$ ceramics as a separator, which was reported [5–7] to be innocuous for the cathode because of high chemical stability, was performed. After that, three kinds of alloy materials were used instead of the LSC separator. The interface between the cathode and the electrolyte was evaluated by electron probe micro analyzer (EPMA, Shimadzu Co. Ltd., EPMA-870) after the half-cell tests. The surface and cross-section of the alloy were analyzed by scanning electron microscope and energy dispersion X-ray analysis (SEM/EDX, JEOL Ltd., EX-23000BU).

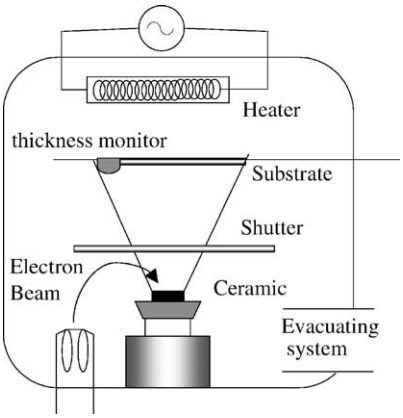

Fig. 2. Schematic illustration of measurement method for Cr-poisoning using a half-cell.

2.3. Single-cell stack test

The stability of single-cell stack performances with LSCO-coated ZMG232 and SUS430 separators were examined. The schematic illustration of the measurement method for a cell stack module is shown in Fig. 3. The cell was manufactured by co-sintering of electrolyte–anode bilayer at 1773 K, followed by firing an interlayer of $Ce_{0.8}Sm_{0.2}O_{1.9}$ (SDC) and a composite of $La_{0.6}Sr_{0.4}Co_{0.2}Fe_{0.8}O_3$/SDC as a cathode. The single-cell was an anode-supported

Table 2
Coating materials and methods

Substrate	Coating material	Thickness (μm)	Coating method
ZMG232	Y_2O_3	~2	Spin coating
ZMG232	La_2O_3	~2	Spin coating
ZMG232	ZnO	~2	Spin coating
ZMG232	$LaAlO_3$	~2	Spin coating
ZMG232	(La,Sr)Co_2O_4	~2	Spin coating
ZMG232	(La,Sr)Co_2O_4	~0.3	EBPVD
ZMG232	(La,Sr)Co_2O_4	~0.6	EBPVD
SUS430	(La,Sr)Co_2O_4	~0.3	EBPVD
SUS430	(La,Sr)Co_2O_4	~0.6	EBPVD

EBPVD: electron beam physical vapor deposition.

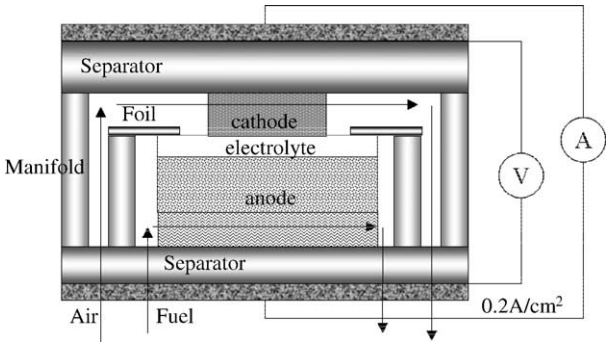

Fig. 3. Schematic illustration of measurement method for a cell stack module.

type having a thin electrolyte, which can be operated at reduced-temperatures. The details of preparing process have been reported in elsewhere [8]. The stack was operated at a current density of 0.2 A/cm^2 at 1023 K using dry hydrogen and air.

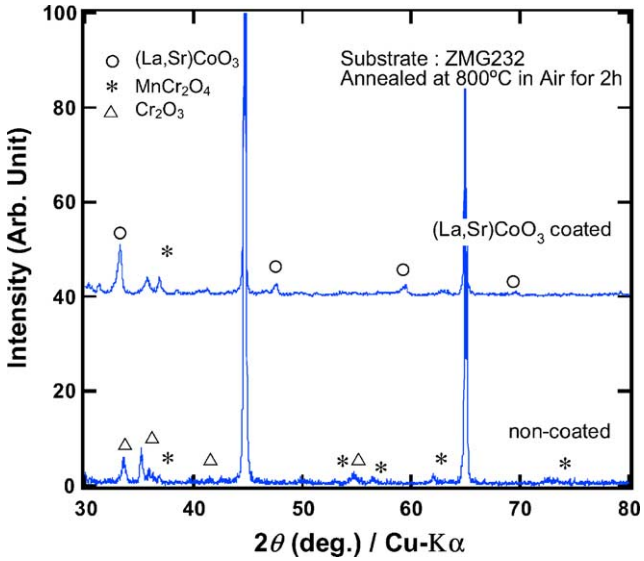

Fig. 5. XRD patterns of non- and LSCO-coated ZMG232.

3. Results and discussion

3.1. Various oxide coating on the ZMG232 alloy

To investigate the degradation of cathode by Cr-poisoning, the half-cell test was conducted with a LSC ceramic separator and alloy separator. Matsuzaki and Yasuda [4,5,9] reported that LSC has high chemical stability and does not deteriorate cathode activity. Fig. 4 shows that the absolute values of the overvoltage (|OV|) decreased gradually with operating time. The decrease could be due to a "current effect." This effect is considered to be caused by a change in the microstructure of the electrode [10], but the details for the mechanism have not been clarified. In the case of the ZMG232 alloy, the |OV| increased rapidly at 7 h. It is considered that the polarization of the cathode increased due to Cr-poisoning. The cathode overvoltage with the YSZ-coated ZMG232 separator was almost equal to that with the LSC ceramic separator. This result indicates that the coating of the alloy is effective to reduce Cr-poisoning. The resistivity of YSZ, however, is too high to be used as a SOFC separator. In the case of the Y_2O_3-coated ZMG232, |OV| increased

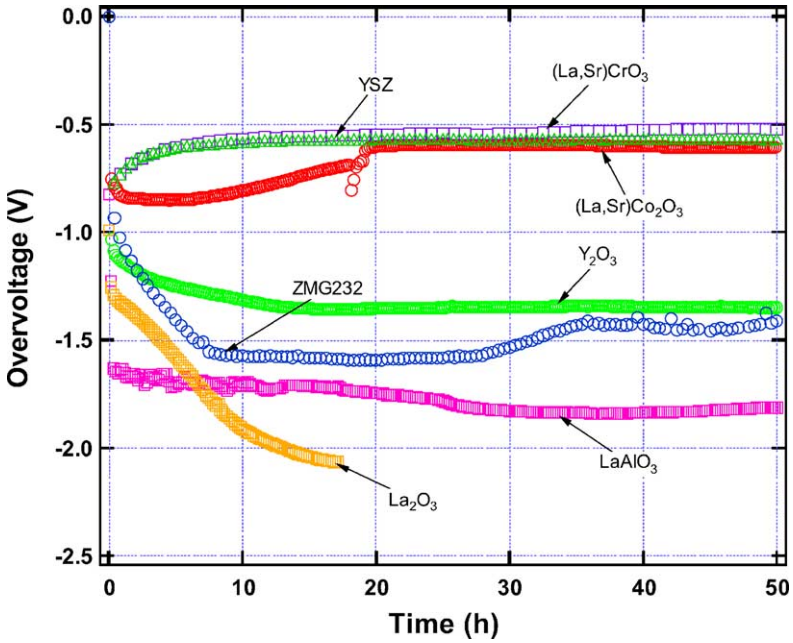

Fig. 4. The effect of coating materials on the degree of Cr-poisoning.

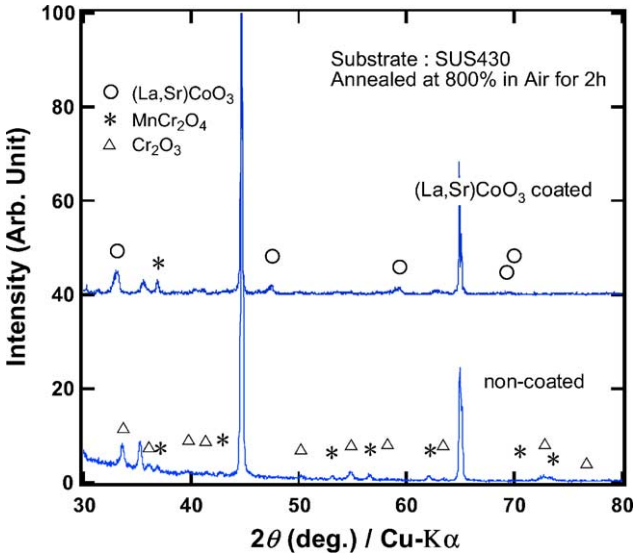

Fig. 6. XRD patterns of non- and LSCO-coated SUS430.

after 20 h, and then remained constant. Thus, the Y_2O_3 coating did not promote the degradation of the cathode, and gave lower |OV| than that of the bare alloy. In the case of the La_2O_3-coated ZMG232, |OV| decreased rapidly. Although the reason was not clarified, it was considered that La_2O_3 could be one of degradation factors. Therefore, it would be important to eliminate unreacted La_2O_3 in the cathode. The ZMG232 separator coated by the $LaAlO_3$ gave a lower degradation than the alloy separator coated by La_2O_3. In the case of LSCO coating, the electrochemical performance of the cathode improved for 20 h, and the performance got closer to that with the LSC ceramic separator. It should be concluded that the LSCO coating is effective to reduce the Cr-poisoning.

3.2. LSCO-coated alloy prepared by EBPVD

3.2.1. XRD patterns of the LSCO coated on alloy substrate

LSCO-coated ZMG232 and SUS430 were annealed in air at 1073 K for 2 h. Figs. 5 and 6 show XRD patterns of the LSCO-coated alloys. The XRD peaks were assigned to LSC and $MnCr_2O_4$, while the peaks of non-coated alloy showed Cr_2O_3 and $MnCr_2O_4$. These results show that the LSCO coating inhibited the growth of Cr_2O_3 on the surface of Cr-containing alloy.

3.2.2. Half-cell test

The effect of the thickness of the LSCO coating on degradation of the cathode by Cr-poisoning was evaluated. Figs. 7 and 8 show the results for ZMG232 and SUS430, respectively. The |OV| of the cathode with coated ZMG232 was smaller than that with non-coated ZMG232. The 3000 Å thick coating of LSCO on SUS430 was effective to reduce |OV|, and the effect increased with the thickness of the LSCO coating. These results indicate that Cr-containing vapor generated from the alloy surface was successfully prevented by the LSCO coating.

3.2.3. Interface between the cathode and the electrolyte after the polarization

The mechanism of the Cr-poisoning can be described by the reactions as follows [11]:

$$\text{Alloy surface}: Cr_2O_3(s) + \tfrac{3}{2}O_2(g) + 2H_2O(g) \rightarrow 2CrO_2(OH)_2(g)$$

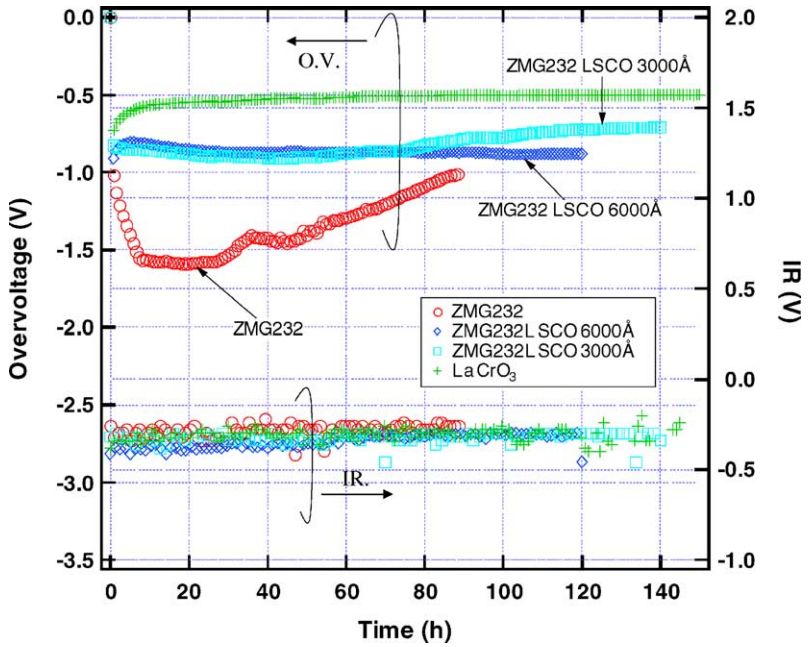

Fig. 7. The effect of LSCO coating on ZMG232 alloy on the degree of Cr-poisoning.

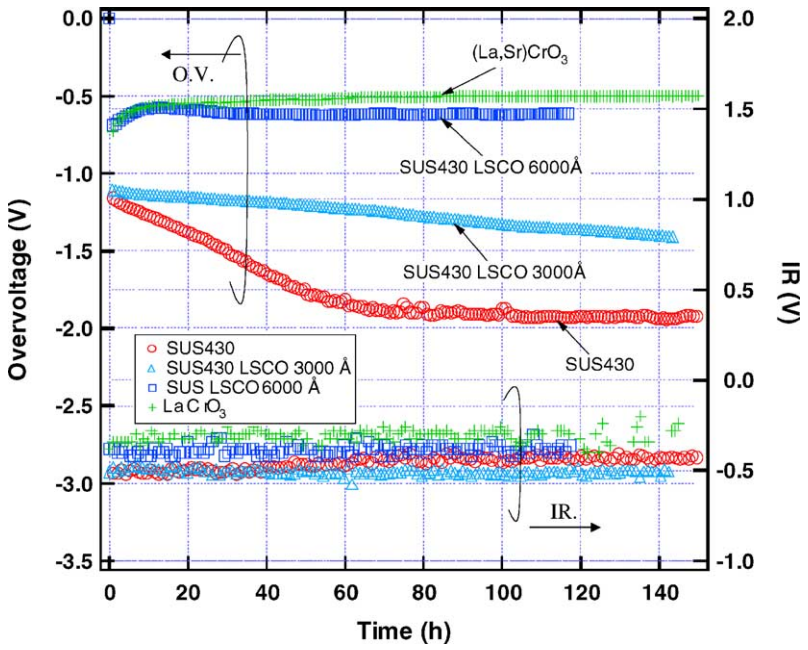

Fig. 8. The effect of LSCO coating on SUS430 alloy on the degree of Cr-poisoning.

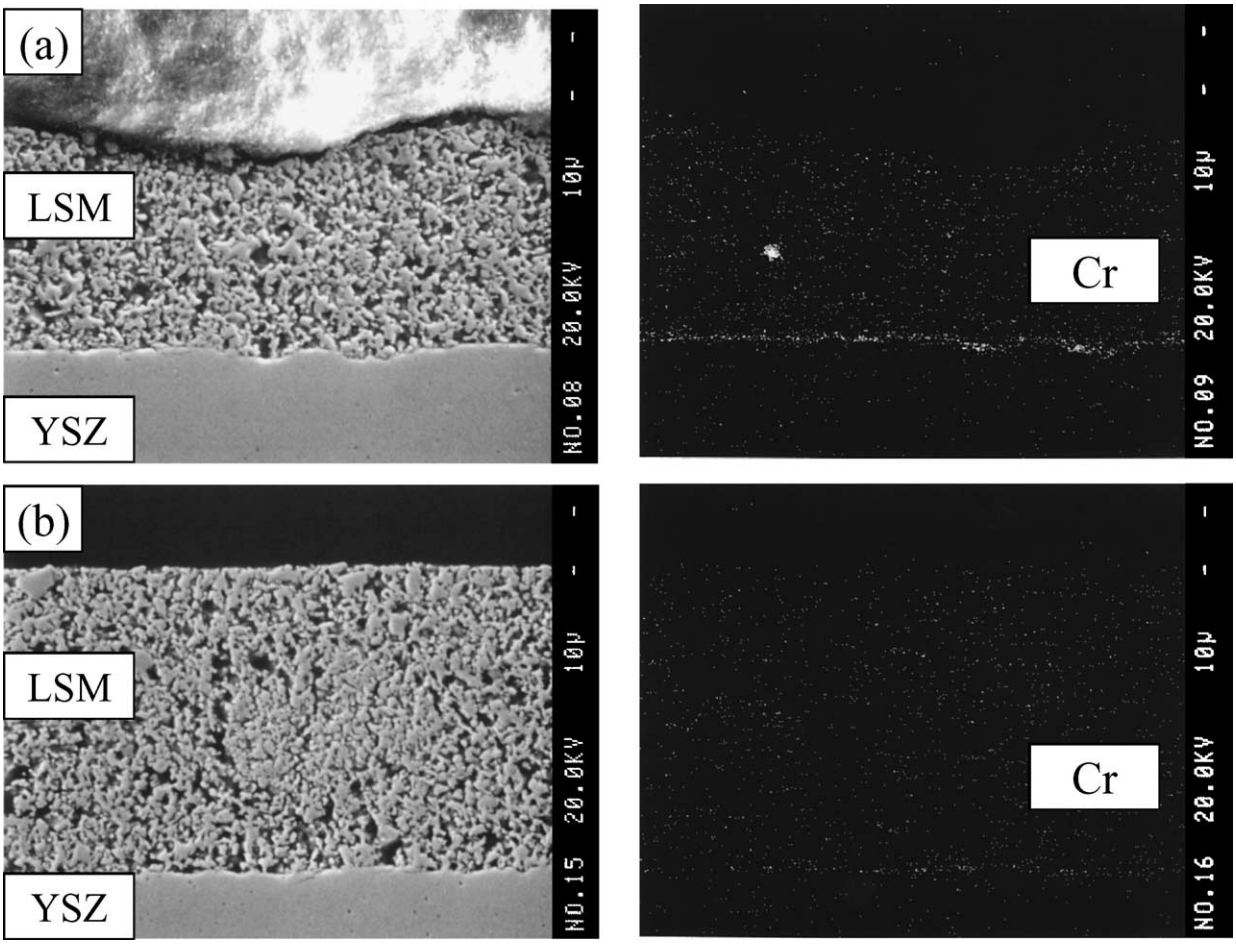

Fig. 9. Cross-sectional SEM/EPMA images of the interface between cathode and electrolyte after the half-cell test using (a) non- and (b) LSCO-coated ZMG232 alloys.

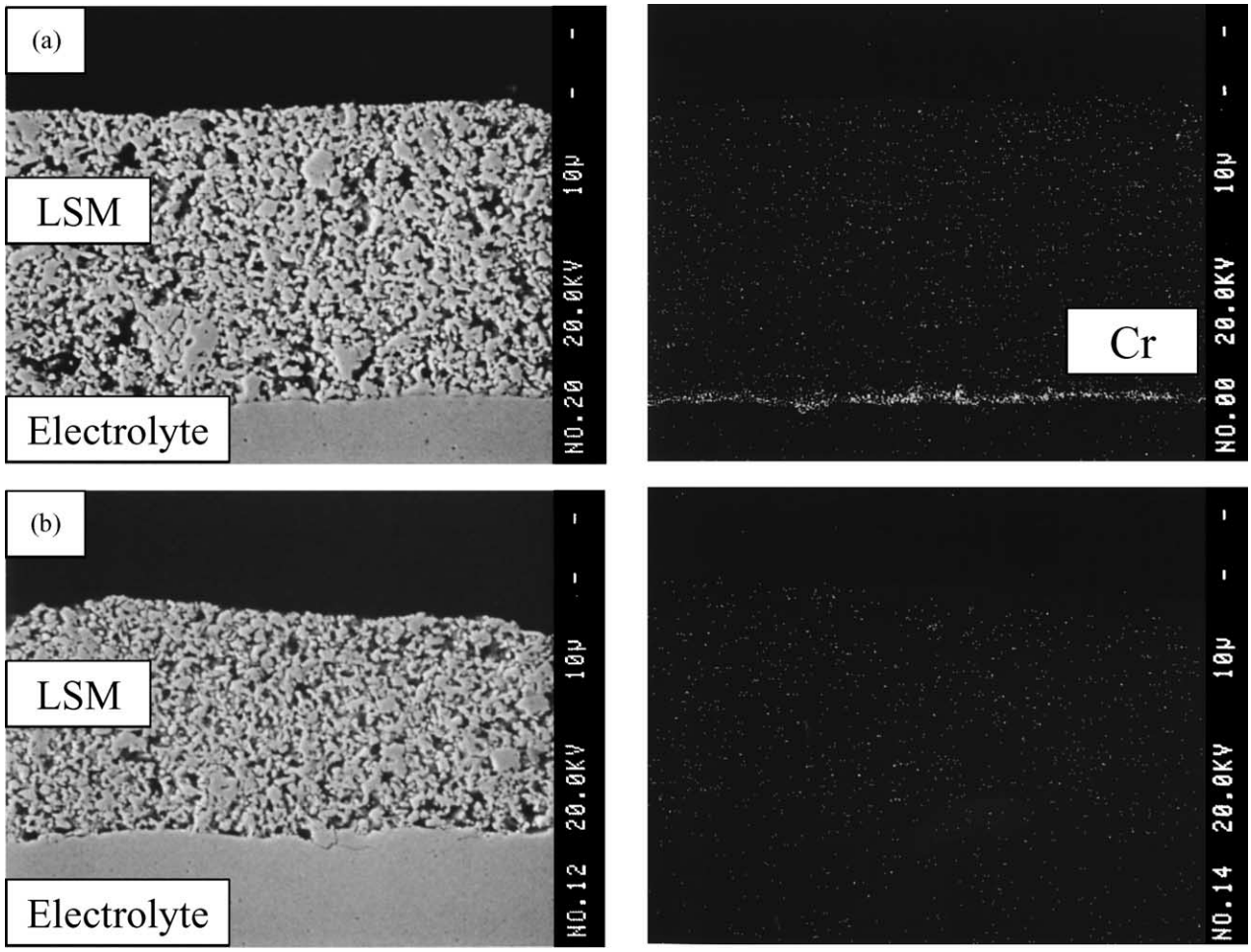

Fig. 10. Cross-sectional SEM/EPMA images of the interface between cathode and electrolyte after the half-cell test using (a) non- and (b) LSCO-coated SUS430 alloys.

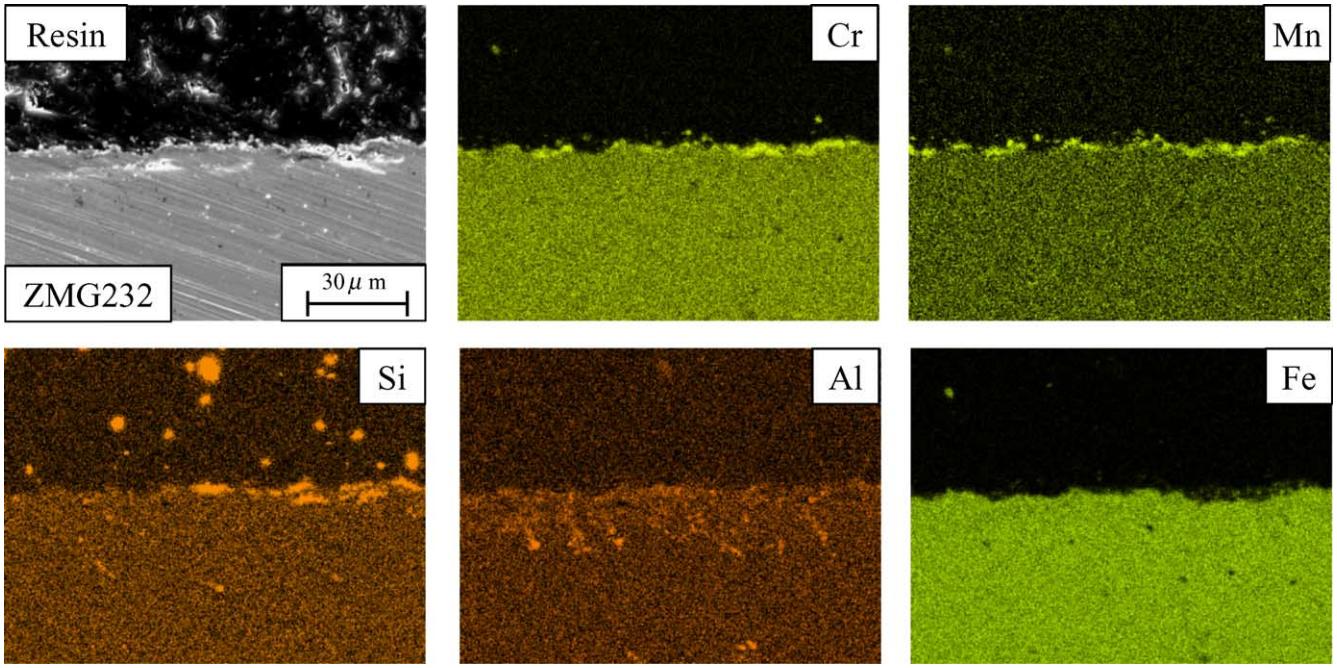

Fig. 11. Cross-sectional SEM/EDX images of oxide layer formed on ZMG232 surface after a polarization for 90 h.

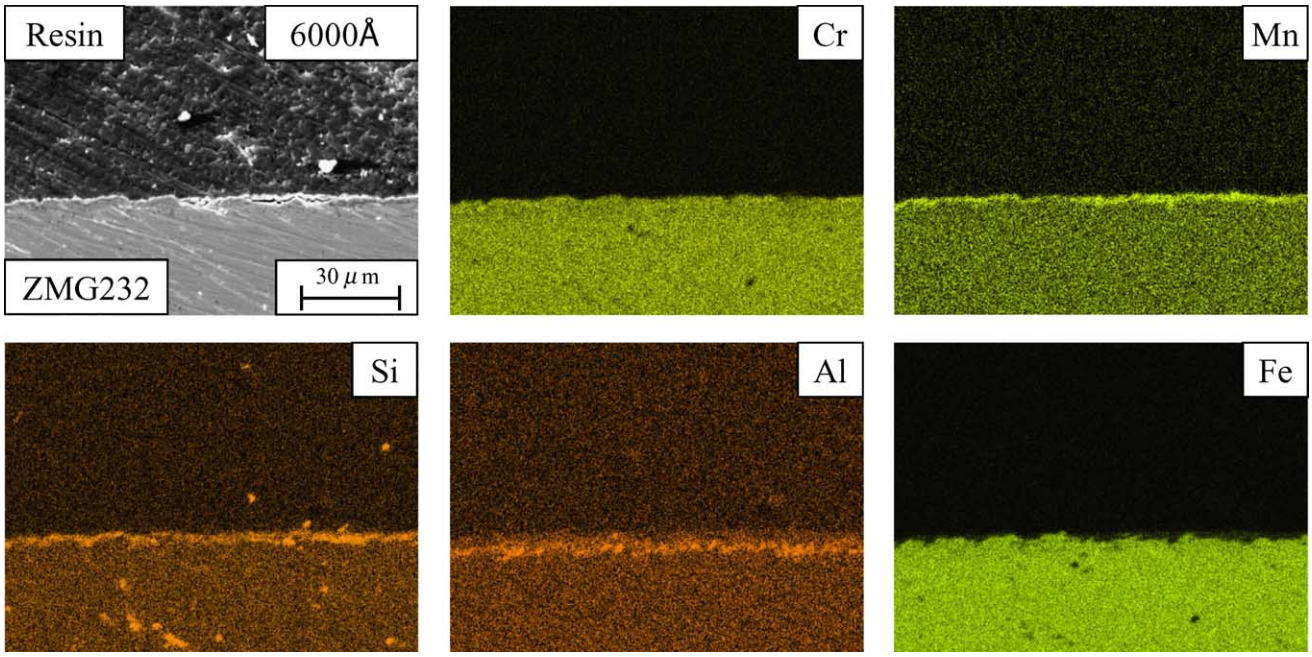

Fig. 12. Cross-sectional SEM/EDX images of oxide layer formed on ZMG232 surface with LSCO coating after a polarization for 140 h.

Cathode/electrolyte interface : $2CrO_2(OH)_2(g) + 6e^-$
$\rightarrow Cr_2O_3(s) + 2H_2O(g) + 3O^{2-}$

According to these reactions the Cr_2O_3 should deposit at the cathode/electrolyte interface. SEM/EDX photographs of the interfaces of half-cells with non- and LSCO-coated alloy after the polarization measurement are shown in Figs. 9 and 10. In the case of LSCO-coated ZMG232 and SUS430, Cr was not detected at the interface. On the other hand, Cr was detected clearly at the interface with non-coated ZMG232. These results support the speculation that the Cr-containing vapor generated from the alloy surface was prevented by the LSCO coating.

3.2.4. Oxide layer of the Cr-containing alloys after polarization

The non- and LSCO-coated alloy separators were analyzed by SEM/EDX. The cross-sectional EDX composition maps of non-coated ZMG232 are shown in Fig. 11. The surface was found to be covered with Cr and Mn. On

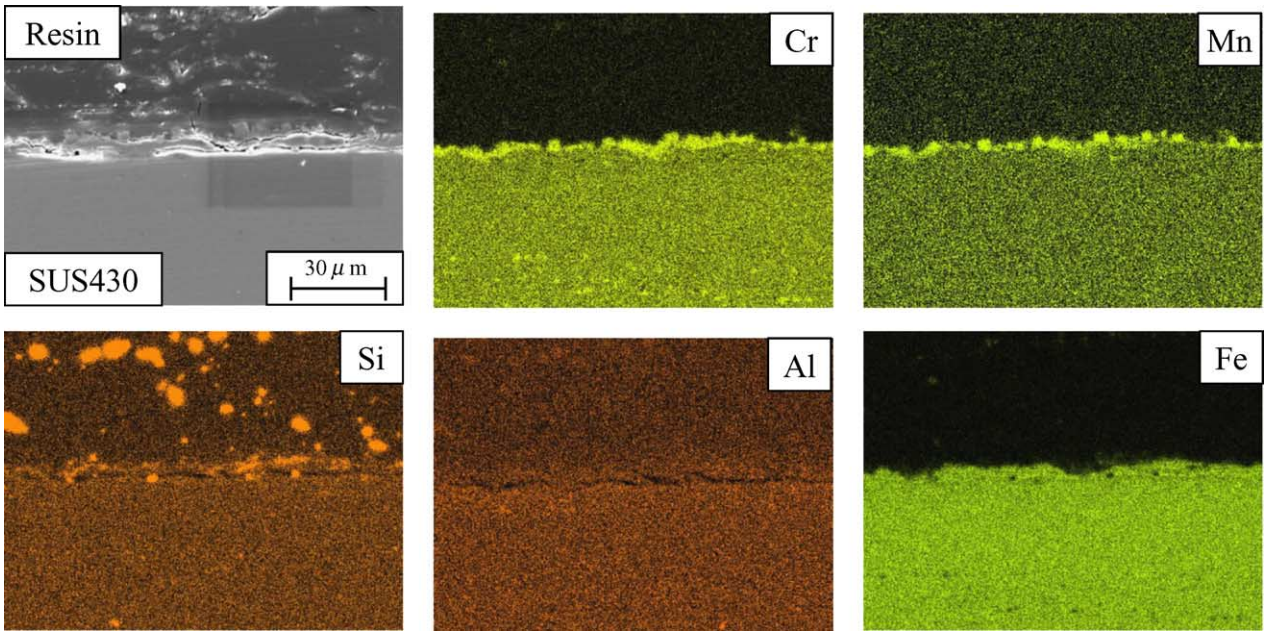

Fig. 13. Cross-sectional SEM/EDX images of oxide layer formed on ZMG232 surface with LSCO coating after a polarization for 120 h.

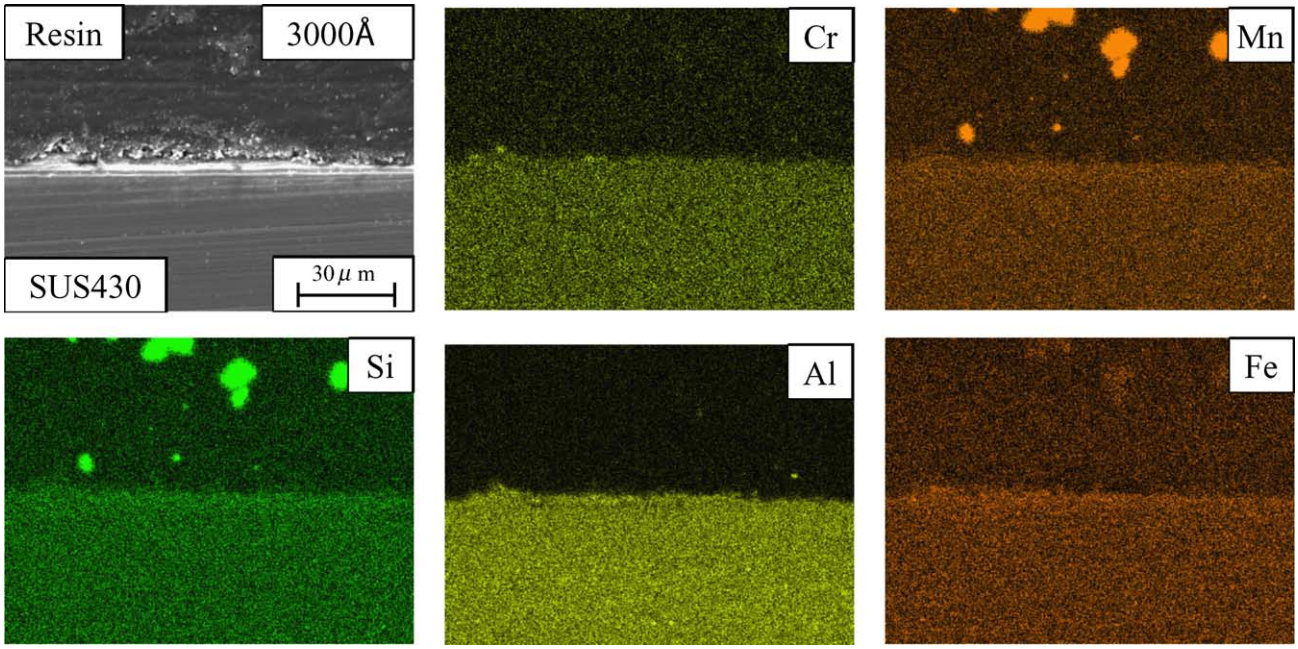

Fig. 14. Cross-sectional SEM/EDX images of oxide layer formed on SUS430 surface after a polarization for 150 h.

Table 3
Chemical compositions of Cr-containing alloy surface layers with or without LSCO coating after half-cell tests

Substrate	Thickness of LSCO coat layer (Å)	Time for half-cell testing (h)	Chemical composition (mol%)						
			Mn	Cr	Fe	Si	Al	La	Co
ZMG232	–	90	15.46	17.21	2.69	0.03	0.24	0.27	0.07
ZMG232	3000	140	18.00	11.09	5.66	0.31	0.12	0.21	3.33
ZMG232	6000	120	12.47	5.66	5.53	0.45	0.16	2.61	8.34
SUS430	–	150	14.22	20.07	3.71	0.11	–	0.29	0.06
SUS430	3000	144	17.64	7.80	3.62	0.24	–	2.84	3.15
SUS430	6000	117	16.18	5.43	3.07	0.12	–	2.86	5.31

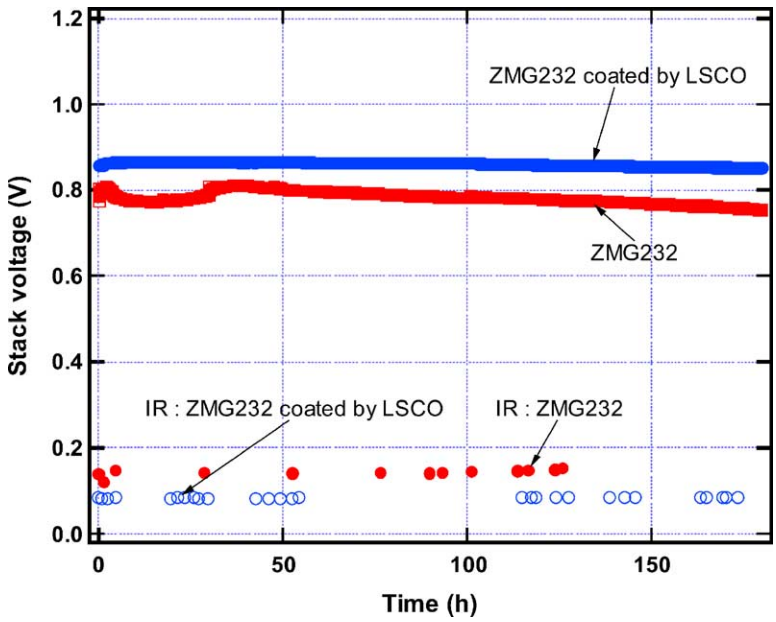

Fig. 15. Cross-sectional SEM/EDX images of oxide layer formed on SUS430 surface with LSCO coating after a polarization for 144 h.

the other hand, Cr was not observed in the EDX image of LSCO-coated ZMG232 as shown in Fig. 12. The same tendency was observed in non- and LSCO-coated SUS430 (Figs. 13–14). The chemical compositions of these alloy surface analyzed by the EDX are listed in Table 3. The amount of Cr on the alloy surfaces was found to decrease by the LSCO coating.

3.2.5. Single-cell stack test

The effect of LSCO coating was examined by single-cell stack tests. Fig. 15 shows time dependencies of the stack voltage using non- and LSCO-coated ZMG232 separators. The voltage with the non-coated separator decreased with time, which is consistent with the result of the half-cell test. On the other hand, the voltage with the LSCO-coated separator was not degraded largely. The cell voltage with non-coated ZMG232 was 0.810 V at 38 h and 0.773 V at 138 h. The rate of degradation was estimated to be as high as 98.8% per 1000 h. The value of LSCO-coated ZMG232 was 0.864 V at 32 h and 0.860 V at 132 h. The estimated rate of degradation was about 4.6% per 1000 h. The long-term stability improved considerably by the LSCO coating.

4. Conclusion

The effects of coated Cr-containing alloy on the Cr-poisoning of SOFC cathode have been investigated. Main results are as follows:

1. LSCO was effective to reduce the growth of Cr_2O_3 on the Cr-containing alloys.
2. The LSCO-coated Cr-containing alloy reduced the Cr-poisoning of the cathode.
3. The LSCO coating of the alloy improved the rate of degradation of the stack voltage.

Acknowledgements

Part of this work was performed as R&D program of New Energy and Development Organization (NEDO). We would like to thank NEDO and Ministry of Economy, Trade and Industry (METI) for their advice and financial support.

References

[1] K. Huanig, P.Y. Hou, J.B. Goodenough, Solid State Ionics 129 (2000) 237.
[2] T. Brylewski, M. Nanko, T. Maruyama, K. Przybylski, Solid State Ionics 143 (2001) 131.
[3] J. Pirón-Abellán, F. Tietz, V. Shemet, A. Gil, T. Ladwein, L. Singheiser, W. Quadakkers, in: Proceedings of Fifth European SOFC Forum, Lucerne, July 2002, p. 248.
[4] Y. Matsuzaki, I. Yasuda, Solid State Ionics 126 (1999) 307.
[5] Y. Matsuzaki, I. Yasuda, Solid State Ionics 132 (2000) 271.
[6] I. Yasuda, T. Hikita, J. Electrochem. Soc. 140 (1993) 1699.
[7] H. Yakabe, M. Hishinuma, I. Yasuda, J. Electrochem. Soc. 147 (2000) 4071.
[8] Y. Matsuzaki, I. Yasuda, Solid State Ionics 152 (2002) 463.
[9] Y. Matsuzaki, I. Yasuda, J. Electrochem. Soc. 148 (2001) 126.
[10] H. Tsukuda, A. Yamashita, K. Hasezaki, J. Ceram. Soc. Jpn. 105 (1997) 862.
[11] S. Taniguchi, M. Kadowaki, T. Yasuo, Y. Akiyama, Y. Itho, Y. Miyake, K. Nishio, Denki Kagaku 64 (1996) 568.